

---

# SEMANTIC AND GEOMETRIC UNFOLDING OF STYLEGAN LATENT SPACE

---

A PREPRINT

**Mustafa Shukor**  
InterDigital, Inc \*

**Xu Yao**  
InterDigital, Inc  
Télécom Paris

**Bharath Bhushan Damodaran**  
InterDigital, Inc

**Pierre Hellier**  
InterDigital, Inc

{firstname.lastname}@interdigital.com

## ABSTRACT

Generative adversarial networks (GANs) have proven to be surprisingly efficient for image editing by inverting and manipulating the latent code corresponding to a natural image. This property emerges from the disentangled nature of the latent space. In this paper, we identify two geometric limitations of such latent space: (a) euclidean distances differ from image perceptual distance, and (b) disentanglement is not optimal and facial attribute separation using linear model is a limiting hypothesis. We thus propose a new method to learn a proxy latent representation using normalizing flows to remedy these limitations, and show that this leads to a more efficient space for face image editing.

## 1 Introduction

GANs [Goodfellow et al. \[2014\]](#) have shown tremendous success in generating high quality realistic images that are indistinguishable from real ones. Yet, several open problems regarding these models still exist, such as image generation control, latent space understanding and attributes disentanglement, which are important for both the generation and editing of high quality images. Recently, many improvements have been proposed to the original GAN architecture [Karras et al. \[2017\]](#), [Brock et al. \[2018\]](#), [Miyato et al. \[2018\]](#), which led to unprecedented image quality [Karras et al. \[2019, 2020\]](#). In particular, the state-of-the-art method StyleGAN [Karras et al. \[2019, 2020\]](#) has been improved, leading to image editing methods using the latent representation [Collins et al. \[2020\]](#), [Shen et al. \[2020a\]](#), [Abdal et al. \[2020\]](#), [Shen et al. \[2020b\]](#). Specifically, recent approaches [Shen et al. \[2020a,b\]](#) assume that the attributes are disentangled and can be separated by hyperplanes, which enables interpolation and one attribute manipulations. InterFaceGAN [Shen et al. \[2020b\]](#) computes an editing direction for each facial attribute, orthogonal to the linear classification boundary for this attribute. We claim that the hyperplane classification boundary assumption is not perfectly true, and the attributes are not perfectly disentangled, which can further explain why these approaches do not lead to perfect attribute manipulation.

We argue that another current limitation of GANs latent space is that the Euclidean distance between two latent codes do not reflect the perceptual distance between the corresponding images. However, distance computation is critical for many applications including facial similarity, image comparison, and data clustering. Designing consistent distances between objects is crucial as shown in [Zhang et al. \[2018\]](#).

The first solution to these limitations could be the retraining of GAN with explicit constraints. However, it is known that the training of GANs is hard and computationally expensive. We propose in this paper an alternative approach without retraining the GAN. Specifically, we will focus on the aforementioned properties and learn a bijective transformation (*i.e.*, Normalizing Flows) from the original latent space (*i.e.*  $\mathcal{W}^+$ ) to a new proxy latent space ( $\mathcal{W}^*$ ). In  $\mathcal{W}^*$ , the facial attributes are linearly separable, disentangled and the latent Euclidean distance mimics the perceptual image distance. The choice of a bijective transformation allows to benefit from the pretrained StyleGAN2 generative capabilities. Figure 1 illustrates the proposed approach. Our contributions are the following:

---

\*Interdigital, Research and Innovation, Rennes, France. The work done during Mustafa's internship.

- We propose to learn a derived latent representation where supervision is used to explicitly disentangle the facial attributes. We also propose to enforce that Euclidean distance in the new latent space mimics the perceptual one in the image space.
- We propose to learn this proxy latent representation using normalizing flows, which can be applied to any pretrained GAN while preserving the generative capability of the original GAN.
- We show experimentally that the desired properties are indeed enforced in this new latent representation, leading to a more efficient image manipulation.

The rest of the paper is organised as follows: section 2 presents related works on GANs, Normalizing Flows, perceptual distances, and attributes disentanglement. Our proposed method is detailed in section 3 and section 4 presents the experimental results and ablation study. Finally, section 5 discusses the approach and conclusions are drawn in section 6. The code will be released once the paper is accepted.

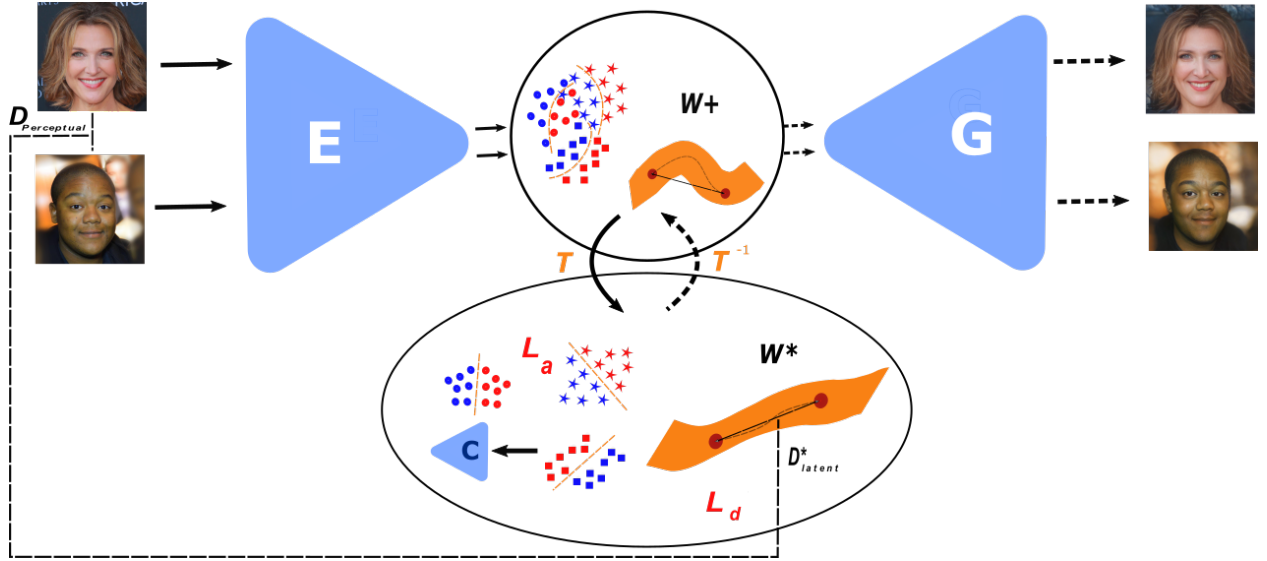


Figure 1: An illustration of our proposed approach.  $E$ ,  $G$ , and  $C$  are the StyleGAN2 encoder, generator and attributes classifier respectively. Only the NF mapping  $T$  is trained. The existing StyleGAN2 latent space  $\mathcal{W}^+$  does not satisfy the linear separability assumption and the consistency between the latent euclidean distance (straight line) and the perceptual distance (dashed geodesic line). In our learned proxy latent space  $\mathcal{W}^*$  the attributes are disentangled, can be separated by hyperplanes (between the positive and negative regions) and the Euclidean latent distance mimics the perceptual distance.

## 2 Related work

**GANs** GANs Goodfellow et al. [2014] are one type of generative models that are trained adversarially to generate complex data distributions starting from a simple one. There are other types such as VAEs Kingma and Welling [2013] and Normalizing Flows Kobayev et al. [2020], though the image quality generated by GANs is higher with reasonable model size. Several improvements have been proposed to improve GANs architecture Radford et al. [2015], loss function Mao et al. [2017], Arjovsky et al. [2017] and its training Gulrajani et al. [2017], Miyato et al. [2018], Karras et al. [2017]. Recently, StyleGAN Karras et al. [2019] was introduced as the state of the art in high-resolution image generation, especially for human faces. This architecture allows better control of the generation process, although it produces some artifacts which were solved in a new version (StyleGAN2 Karras et al. [2020]). The latent space of StyleGAN2 ( $\mathcal{W}$ ) is better disentangled than the original  $\mathcal{Z}$  space. Furthermore, the  $\mathcal{W}^+$  is better for image editing Abdal et al. [2019], Xu et al. [2020], Wei et al. [2021] and the focus in our work is to obtain a new space with better properties.

**Disentangled Representations** There have been many efforts to obtain disentangled representation for generative models (e.g., VAEs and GANs). In  $\beta$ -VAE Higgins et al. [2017] they put a strong constraint to obtain latent posterior

distribution with uncorrelated dimensions. Similarly, FactorVAE Kim and Mnih [2018] minimizes the total correlation (TC) of the latent space distribution to encourage independence. InfoGAN Chen et al. [2016] maximizes the mutual information between a small subset of the latent dimensions and the generator distribution. This is improved in InfoGAN-CR Lin et al. [2019], where each dimension in the latent code is encouraged to make a significant change to the image. Recently, Zheng et al. Zheng et al. [2021] leverage an auxiliary task (*i.e.* face reconstruction) and a decorrelation loss to obtain disentanglement. All these approaches require retraining the generator. In addition, they are unsupervised which limits the range of attributes that they can manipulate, for instance, we can change the age, gender and adding makeup while in all these mentioned methods it is not clear how to achieve such manipulation.

**Normalizing Flows (NFs)** NFs Kobyzev et al. [2020] are another type of generative models that consists of diffeomorphic transformations between a simple known distribution and any arbitrarily complex one. Due to the constraints that should be satisfied (*e.g.* bijectivity, tractable inverse and jacobian determinant) the expressivity of such models is limited compared to others (*e.g.* GANs). In recent years, there have been many attempts to improve them. Real NVP Dinh et al. [2016] is one of the Discrete NF models that was able to generate good quality images. MAF Papamakarios et al. [2017] was also proposed but it is not efficient as Real NVP as it is not parallelizable. Recently, Glow Kingma and Dhariwal [2018] was proposed as the state of the art in high quality image generation. Unfortunately, its success depends on a very large number of parameters, making this model difficult to train in practice. Continuous NF Grathwohl et al. [2018] has been proposed, which usually gives comparable expressivity to DNF with smaller models. However, since it is based on ODE solver, the inference is computationally demanding for real time applications such as video editing.

**Perceptual distances** Computing image distance that is consistent with the human perception is of high interest for many computer vision applications. As the traditional L1/L2 distances do not have this property, many works were devoted to handcraft perceptual distances Zhao et al. [2017], Sims [2020]. Recently, VGG16 Johnson et al. [2016] was one of the first feature based distances that outperforms all the handcrafted ones. It consists of computing the L2 distance between the features extracted from a pretrained VGG16 network. This was followed by LPIPS Zhang et al. [2018] which uses a pre-trained network fine-tuned on perceptual judgement prediction task. Some perceptual distances were designed for specific tasks Mustafa et al. [2021].

### 3 Method

In this section, we explain how to learn a proxy latent space (dubbed  $\mathcal{W}^*$ ) that satisfies two properties: (a) a latent Euclidean distance that mimics the perceptual one in the image space (Sec 3.1) and (b) disentanglement and linear separation of the attributes (Sec 3.2). In addition, we will explain how other properties that are useful for image editing can be satisfied.

We assume that we have a pretrained StyleGAN2 generator  $G$  that considers a latent code  $w \in \mathcal{W}^+$  and generates a high resolution image  $I$  (*i.e.* , 1024 x 1024). A bijective transformation  $T : \mathcal{W}^+ \rightarrow \mathcal{W}^*$  is trained to map a latent code  $w \in \mathcal{W}^+$  to  $w^* \in \mathcal{W}^*$ .  $T$  is a Normalizing Flows (NFs) model and can be inverted explicitly. The focus of our work is on real natural images, thus we assume that there exists a pretrained encoder  $E$  that embeds any image in  $\mathcal{W}^+$  such that  $G(E(I)) \simeq I$ . Although, the transformation  $T$  is modelled as a NF, it is noted that our work only requires the bijectivity, as such, we did not impose the prior distribution in the proxy latent space as we are not interested in the density estimation.

#### 3.1 Latent Distance Unfolding

The objective here is to learn the mapping  $T$  that maps the latent codes to the new latent space such that the latent distance in this space is similar to the perceptual one in the image space. This property is obtained by minimizing the distance between the proxy latent distance and perceptual distance as below:

$$\mathcal{L}_d = \frac{1}{N-1} \sum_{i,j \in S} (\|T(E(I_i)) - T(E(I_j))\|_2^2 - D_{perceptual}(I_i, I_j))^2 \quad (1)$$

where  $S$  is a set of image samples indices of size  $N$ . The first term is the latent squared Euclidean distance in  $\mathcal{W}^*$  ( $D_{latent}^*(\cdot, \cdot)$ ) and  $D_{perceptual}(\cdot, \cdot)$  is the perceptual distance.  $D_{perceptual}$  could be any perceptual distance. We refer to the latent distance in  $\mathcal{W}^+$  as  $D_{latent}$ .

### 3.2 Attributes Disentanglement

The main objective here is to learn  $T$  that maps the latent codes to the new space where the linear classification is optimal for each attribute. This is done by minimizing the classification loss of a linear attribute classifier  $C : \mathcal{W}^* \rightarrow \{0, 1\}^K$ , where  $K$  is the number of attributes labeled in the image dataset. Choosing a linear model is mainly to enforce the linear separation between the positive and negative regions of each attribute while reducing the loss in general leads to better attributes disentanglement. Instead of using one classification model for all the attributes, we found that it is better to use one binary classification model for each attribute and train these models jointly. For each sample  $w$ , the objective is to minimize:

$$\mathcal{L}_a = - \sum_{i=0}^K y_i \log(C_i(T(w))) + (1 - y_i) \log(1 - C_i(T(w))) \quad (2)$$

Where  $C_i : \mathcal{W}^* \rightarrow \{0, 1\}$  is the classifier for the  $i$ th attribute,  $y_i \in \{0, 1\}$  is the label of the sample  $w$  corresponding to the  $i$ th attribute. In (2) the classifiers are fixed and only  $T$  is optimized as we are interested in obtaining a linear separation for each attribute. Theoretically, any linear classifier could be used. However, since a form of linear separation already exists in  $\mathcal{W}^+$ , we choose to pretrain the linear classifiers first in  $\mathcal{W}^+$  and fix it while optimizing for  $T$ . This provides some regularization so that  $T$  only focuses on improving the pre-trained classifier. In addition, it helps to converge faster.

Our proposed proxy latent space  $\mathcal{W}^*$  with both properties; the attributes disentanglement/separation and latent distance unfolding are learned by minimizing the joint loss as:

$$\mathcal{L}_{\mathcal{W}^*} = \mathcal{L}_a + \lambda_d \mathcal{L}_d, \quad (3)$$

where  $\lambda_d$  trade-off between the two losses.

### 3.3 Regularization for Image Editing

Specifically for image editing, we introduce additional regularizations in (3) to better condition the properties of  $\mathcal{W}^*$ . For instance, it is important to preserve the person identity after editing. Identity preservation is enforced by minimizing the loss between the features extracted from a pretrained face recognition model  $F$  before and after editing. Thus for a given image sample  $I$ , the identity preservation loss can be written as:

$$\mathcal{L}_{ID} = \|F(G(E(I))) - F(G(T^{-1}(T(E(I)) + \epsilon))\|_2^2 \quad (4)$$

where  $\epsilon \sim \mathcal{N}(0, I)$  accounts for noise or image manipulation. Thus the total loss with identity regularization is written as follows:

$$\mathcal{L}_{\mathcal{W}_{ID}^*} = \mathcal{L}_a + \lambda_d \mathcal{L}_d + \lambda_{ID} \mathcal{L}_{ID} \quad (5)$$

where  $\lambda_d$  and  $\lambda_{ID}$  are the weights of the respective loss terms.

## 4 Experiments

In this section we evaluate the properties of our proposed proxy latent space  $\mathcal{W}^*$ . First, we detail the implementation details, next we describe the quantitative metrics, and finally we present the experimental results.

### 4.1 Implementation Details

We use a pretrained StyleGAN2 ( $G$ ) on FFHQ dataset [Karras et al. \[2019\]](#). The images are encoded in  $\mathcal{W}^+$  using a pretrained StyleGAN2 encoder ( $E$ ) [Richardson et al. \[2020\]](#) (the parameters of the generator and the encoder remain fixed in all the experiments). The latent vector dimension in  $\mathcal{W}^+$  and  $\mathcal{W}^*$  is  $18 \times 512$ . Celeba-HQ [Karras et al. \[2017\]](#) is the image dataset that is used and consists of 30000 high quality images (*i.e.* 1024x1024) of faces where each image has annotation for  $K = 40$  attributes. A single layer MLP model for each attribute ( $C_i$ ) is used as linear classifier which is pretrained in  $\mathcal{W}^+$ . For the NF model, Real NVP [Dinh et al. \[2016\]](#) is used without batch normalization. Each coupling layer consists of 3 fully connected (FC) layers for the translation function and 3 FC for the scale one with LeakyReLU as hidden activation and Tanh as output one. VGG16 [Johnson et al. \[2016\]](#) features of blocks 2, 3 and 4, pretrained on Imagenet is used to compute perceptual distance. For the face recognition model  $F$  we use VGG16 pretrained on a face recognition dataset [Parkhi et al. \[2015\]](#). For all the experiments, Adam optimizer is used with  $\beta_1 = 0.9$  and  $\beta_2 = 0.999$ , learning rate= $1e-4$  and the batch size=8.



Space	Linear separation			Disentanglement			Dist. Unfolding		
	Min Class. Acc $\uparrow$	Max Class. Acc $\uparrow$	Avg. Class. Acc $\uparrow$	D $\uparrow$	C $\uparrow$	I $\downarrow$	Mean $\downarrow$	STD $\downarrow$	2AFC $\uparrow$ score
$\mathcal{W}^+$	0.635	0.979	0.834	0.59	0.43	0.30	-1.185	0.970	0.58
$\mathcal{W}^*$	<b>0.822</b>	<b>0.989</b>	<b>0.913</b>	<b>0.75</b>	<b>0.52</b>	<b>0.27</b>	<b>0.035</b>	<b>0.384</b>	<b>0.83</b>

Table 1: The quantitative assessment of the attribute’s linear separation, disentanglement and latent distance unfolding in the  $\mathcal{W}^+$  and  $\mathcal{W}^*$ . The  $\uparrow$  ( $\downarrow$ ) indicates the higher (lower) values are better and the best results in **bold**. We can notice that in  $\mathcal{W}^*$ ; the latent distance is closer to the perceptual distance and the attributes are more disentangled and linearly separable.

## 4.2 Quantitative metrics

To assess the linear separation and disentanglement for attributes we use classification accuracy and DCI Eastwood and Williams [2018], and for latent distance unfolding we use 2AFC score and some statistics.

**Classification Accuracy:** An SVM was trained from scratch for each attribute on 15000 latent codes in the corresponding space. In  $\mathcal{W}^+$  the latent codes were obtained after encoding the images of Celeba-HQ using the pretrained encoder, and in  $\mathcal{W}^*$  were obtained after mapping the encoded codes using the trained NF model  $T$ . Among the available latent codes, we split 80% for training and the rest of them for validation. The accuracy measures are reported using minimum classification accuracy (Min Class.Acc), maximum classification accuracy (Max Class.Acc) among the attributes and average accuracy (Avg Class.Acc).

**DCI Eastwood and Williams [2018]:** DCI is used to assess disentanglement; Disentanglement (D) quantifies how much each dimension captures at most one attribute, Completeness (C) quantifies how much each attribute is captured by a single dimension and Informativeness (I) quantifies how much informative the latent code is for the attributes which is simply the classification error. We have used 40 Lasso regressors from scikit-learn library with  $\alpha = 0.02$  that is multiplied by the L1 regularizer. The dataset size is 2000 which is composed of the validation set of Celeba-HQ encoded using the pretrained encoder. The train and validation sets are splitted as 80% and 20% respectively. The regressors are trained using the RMSE loss.

**Mean, STD:** To measure how much the latent distance deviates from perceptual distance, we report the mean and standard deviation of the difference between the latent and perceptual distances (Mean and STD). In order to compute this, we randomly sampled 600 pairs of latent codes (images are from the Celeba-HQ dataset and were encoded using the pretrained encoder) and computed the latent distance in both spaces ( $\mathcal{W}^+$  and  $\mathcal{W}^*$ ) and the perceptual distance of the corresponding image pairs.

**2AFC score:** 2AFC test Zhang et al. [2018] consists of choosing which of the two distorted images (*i.e.* I0, I1) is more similar to the reference one. In our case, the 3 images were selected at random from Celeba-HQ dataset, encoded using the pretrained encoder, and the latent distance was computed between the 2 pairs. The ground truth was obtained based on the judgment of the VGG16 perceptual distance pretrained on Imagenet. The 2AFC score is computed as the number of right decisions divided by the total number of triplets.

## 4.3 Results

### 4.3.1 Attributes Disentanglement and Latent Distance Unfolding

In this experiment, Real NVP consists of 13 coupling layers and we set  $\lambda_d = 10$  in eq. (3). The classifier  $C$  is pretrained in  $\mathcal{W}^+$  and fixed to benefit from the properties of  $\mathcal{W}^+$ . For this reason, we do not use batch normalization in the Real NVP, otherwise batch normalization normalizes the data and the hyperplanes of the pretrained classifiers will not hold. Table 1 reports the quantitative metrics in  $\mathcal{W}^*$  and  $\mathcal{W}^+$ . When the attributes disentanglement is considered, we can notice a significant improvement in the classification accuracy and DCI metrics in  $\mathcal{W}^*$  over  $\mathcal{W}^+$ . For example, the latent space  $\mathcal{W}^*$  is improved by 20% with respect to the minimum classification accuracy. This demonstrates that in our proposed proxy latent space the linear separability of attributes is better and similar observation also holds for attributes disentanglement. On the other hand, when the latent distance is considered, the mean and std reveals that the Euclidean distance in  $\mathcal{W}^+$  is inconsistent with perceptual distance in the image space, whereas in  $\mathcal{W}^*$  it mimics better the perceptual distance (also check supplementary material). Further, the 2AFC score demonstrates that the latent

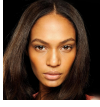





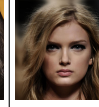


	I 0	Ref	I 1	I 0	Ref	I 1	I 0	Ref	I 1
									
$D_{perceptual}$			✓			✓	✓		
$D_{latent}$	✓			✓					✓
$D_{latent}^*$ (ours)			✓			✓	✓		

Figure 2: 2AFC results on the triplets (middle reference image, on the left and right are the images to be compared with the reference one).  $D_{perceptual}$ ,  $D_{latent}$ , and  $D_{latent}^*$  are the VGG16 perceptual distance, Euclidean latent distance in  $\mathcal{W}^+$  and  $\mathcal{W}^*$  respectively. Compared to the distance computed in  $\mathcal{W}^+$ , the distance in  $\mathcal{W}^*$  agrees with the perceptual one.

distance  $D_{latent}^*$  in  $\mathcal{W}^*$  is significantly higher with large margin than in  $\mathcal{W}^+$  and also Figure 2 shows  $D_{latent}^*$  mimics the human perception.

#### 4.3.2 Image Editing

Here we qualitatively demonstrate the benefits of the new proxy space for the image editing task. InterFaceGAN Shen et al. [2020b] was retrained to manipulate the attributes of a given real image in both  $\mathcal{W}^+$  and  $\mathcal{W}_{ID}^*$  (eq. (5) was optimised). InterFaceGAN assumes that the positive and negative examples of each attribute are linearly separable, and the editing direction is simply the normal to the hyperplane that separates the positive and negative regions. These normal directions were obtained after training an SVM for each attribute in both spaces. The edited images were generated after editing the latent codes in  $\mathcal{W}^+$  or  $\mathcal{W}_{ID}^*$  before feeding them to the StyleGAN2 generator. For  $\mathcal{W}_{ID}^*$ , the edited latent codes were mapped back to  $\mathcal{W}^+$  before feeding them to the generator.

**Implementation details:** Real NVP consists of 3 coupling layers without batch normalization and the loss function was minimized with identity preserving loss (5). The same setup as in 4.1 was adopted. The editing directions were obtained after training an SVM on 15000 images of Celeba-HQ encoded using the pretrained encoder in  $\mathcal{W}^+$  and  $\mathcal{W}_{ID}^*$ . The editing step is 6 for  $\mathcal{W}^+$  and it is between 10 to 15 for  $\mathcal{W}_{ID}^*$  (Note that with higher step the identity changes and the attributes become less disentangled). The model is trained on a Tesla V100 GPU (32GB) for 9 hours.

**Results:** Figure 3 displays the editing results on five attributes in  $\mathcal{W}_{ID}^*$  and  $\mathcal{W}^+$  and it shows that the editing results are visually better in  $\mathcal{W}_{ID}^*$  than in  $\mathcal{W}^+$ . In particular, we see the following observation in  $\mathcal{W}^+$ : gender is still entangled with adding Makeup and Lipstick (3rd row where the male gender is changed to female), changing the gender to Male is entangled with adding Beard and the Hair (column 4), and adding Mustache is entangled with gender (row 5). While in  $\mathcal{W}_{ID}^*$  these attributes are better disentangled and the identity is better preserved. Finally, it is clear that we still obtain high quality images even if we did not retrain the generator and the editing is not done in  $\mathcal{W}^+$ .

Space	Linear separation			Disentanglement			Dist. Unfolding	
	Min Class. Acc ↑	Max Class. Acc ↑	Avg. Class. Acc ↑	D ↑	C ↑	I ↓	Mean ↓	STD ↓
$\mathcal{W}^*$ (H)	<b>0.787</b>	0.991	<b>0.928</b>	<b>0.82</b>	<b>0.56</b>	0.27	0.17	0.15
$\mathcal{W}^*$ (L)	0.777	<b>0.992</b>	0.913	0.81	0.55	<b>0.26</b>	0.13	0.14

Table 2: Ablation study of model architecture.  $\mathcal{W}^*$  (H) and  $\mathcal{W}^*$  (L) refer to Real NVP model with 13 and 3 coupling layers, respectively. Although the classification accuracy and the disentanglement metric show slightly better results in  $\mathcal{W}^*$  (H), the difference is not significant, advocating to retain the model with the smallest capacity.

#### 4.3.3 Ablation Study

In this section, we present the ablation study for attributes separation, distance unfolding and image editing. Implementation details and more results can be found in the suppl. material.

**Attribute’s separation and distance unfolding:** To assess the sensitivity of our proposed method with the number of coupling layers, we conducted experiments with higher and lower Real NVP model capacity and the results (Table 3) shows that higher capacity model  $\mathcal{W}^*$  (H) are slightly better than lower capacity one  $\mathcal{W}^*$  (L).

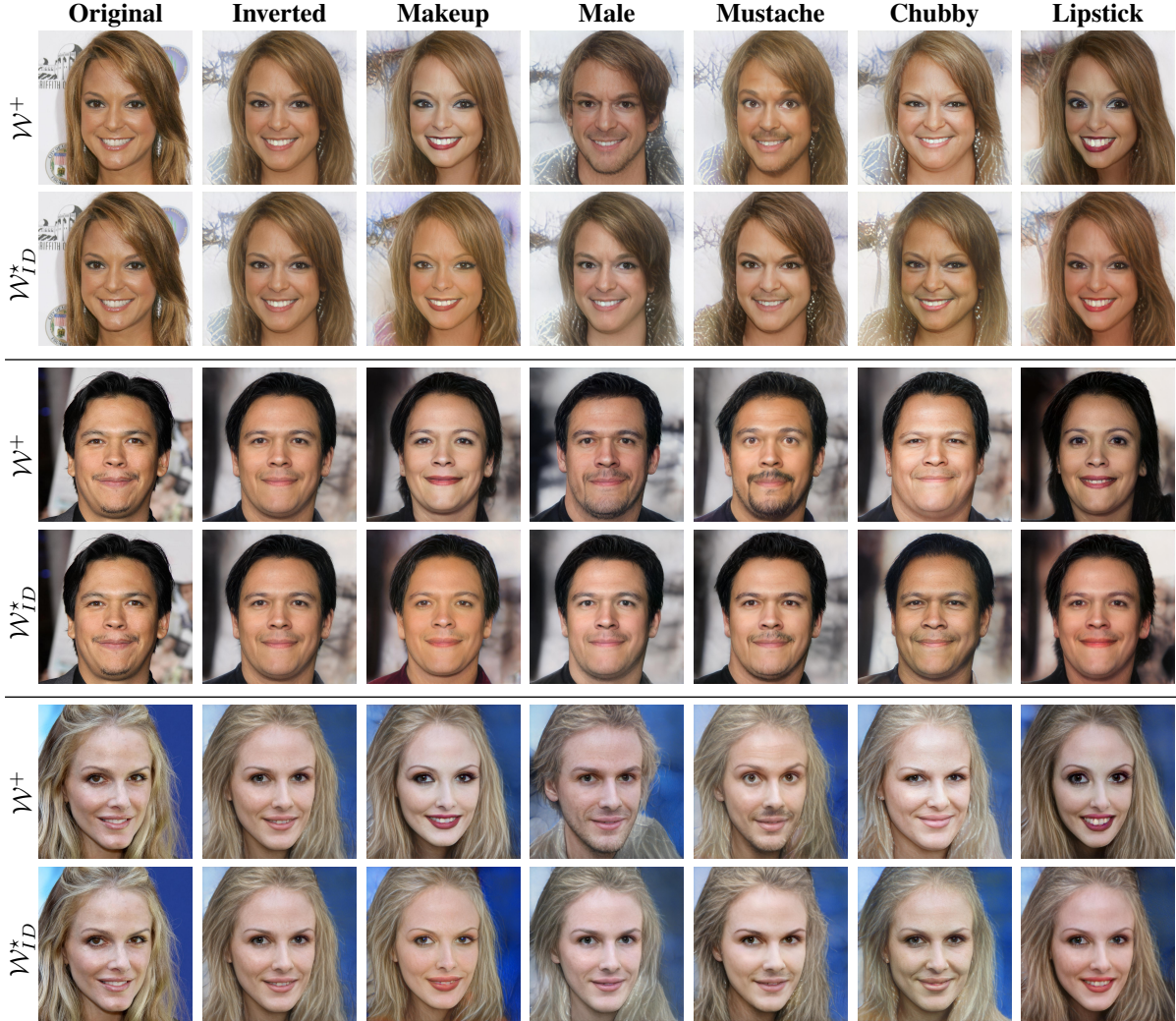


Figure 3: Image editing at resolution  $1024^2$  using InterFaceGAN in  $\mathcal{W}^+$  and  $\mathcal{W}_{ID}^*$ : The images are projected in the latent space of StyleGAN2, then the latent codes are moved in the direction that corresponds to changing one facial attribute. The editing is better in terms of attributes disentanglement in the new learned space ( $\mathcal{W}_{ID}^*$ ) compared to the editing done in the original latent space ( $\mathcal{W}^+$ ). Our method also leads to a better identity preservation.

**Image Editing:** In Figure 8, We can notice that the identity preservation loss helps indeed to preserve subject’s identity and leads to a higher quality image editing. The latent distance unfolding loss benefit is less significant for editing.

## 5 Discussion

Our proposed method has enforced the linear separability and attribute disentanglement for image editing. Although other properties could be considered as well (*e.g.*, pose preservation). Note that, these valuable properties could not be achieved in the original latent space without retraining the encoder and the generator. At the same time, we succeeded to unfold the distance in such a way that the latent Euclidean distance approximates the perceptual VGG16 distance. This method is generic and could be used for any perceptual or hand-crafted distance. We believe that this approach is useful when a specific distance is better than the latent Euclidean distance for a given application. In addition, our attribute separation approach could be extended in a straightforward way to other types of models (*e.g.* VAEs, GANs) that manipulate the images in their latent space. For distance unfolding, the scope of models is larger as any model with a latent space could be adopted.



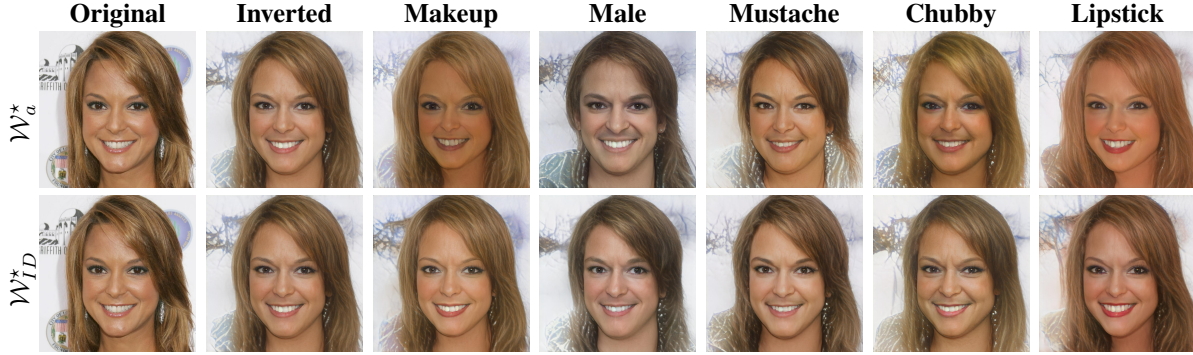


Figure 4: Ablation study of Image editing using InterFaceGAN. Top row: model trained with only the attribute separation loss  $\mathcal{W}_a^*$ . The attribute separation loss alone is clearly not sufficient to obtain a controllable and identity-preserving editing.

## 6 Conclusion

We presented a general framework to enforce additional geometric and semantic properties to the latent space of generative models without the burden of retraining them. In particular, we trained a bijective transformation from the extended space of StyleGAN2 ( $\mathcal{W}^+$ ) to a proxy space ( $\mathcal{W}^*$ ) where two properties are satisfied; the attributes are disentangled and the latent distance mimics the perceptual one in the image space. This generic method enables to bring additional supervision and regularization on top of any trained GAN. We validated our approach by surpassing the original latent space in terms of quantitative metrics and by showing better editing results in terms of attributes disentanglement. We plan to leverage this space for future applications that are affected by a well-conditioned latent distance.

## References

- Rameen Abdal, Yipeng Qin, and Peter Wonka. Image2stylegan: How to embed images into the stylegan latent space? In *Proceedings of the IEEE/CVF International Conference on Computer Vision*, pages 4432–4441, 2019.
- Rameen Abdal, Yipeng Qin, and Peter Wonka. Image2stylegan++: How to edit the embedded images? In *Proceedings of the IEEE/CVF Conference on Computer Vision and Pattern Recognition*, pages 8296–8305, 2020.
- Martin Arjovsky, Soumith Chintala, and Léon Bottou. Wasserstein generative adversarial networks. In Doina Precup and Yee Whye Teh, editors, *Proceedings of the 34th International Conference on Machine Learning*, volume 70 of *Proceedings of Machine Learning Research*, pages 214–223. PMLR, 06–11 Aug 2017. URL <http://proceedings.mlr.press/v70/arjovsky17a.html>.
- Andrew Brock, Jeff Donahue, and Karen Simonyan. Large scale gan training for high fidelity natural image synthesis. *arXiv preprint arXiv:1809.11096*, 2018.
- Xi Chen, Yan Duan, Rein Houthoofd, John Schulman, Ilya Sutskever, and Pieter Abbeel. Infogan: Interpretable representation learning by information maximizing generative adversarial nets. *arXiv preprint arXiv:1606.03657*, 2016.
- Edo Collins, Raja Bala, Bob Price, and Sabine Susstrunk. Editing in style: Uncovering the local semantics of gans. In *Proceedings of the IEEE/CVF Conference on Computer Vision and Pattern Recognition*, pages 5771–5780, 2020.
- Laurent Dinh, Jascha Sohl-Dickstein, and Samy Bengio. Density estimation using real nvp. *arXiv preprint arXiv:1605.08803*, 2016.
- C. Eastwood and C. K. Williams. A framework for the quantitative evaluation of disentangled representations. In *ICLR*, 2018.
- Ian J Goodfellow, Jean Pouget-Abadie, Mehdi Mirza, Bing Xu, David Warde-Farley, Sherjil Ozair, Aaron Courville, and Yoshua Bengio. Generative adversarial networks. *arXiv preprint arXiv:1406.2661*, 2014.
- Will Grathwohl, Ricky TQ Chen, Jesse Bettencourt, Ilya Sutskever, and David Duvenaud. Ffjord: Free-form continuous dynamics for scalable reversible generative models. *arXiv preprint arXiv:1810.01367*, 2018.
- Ishaan Gulrajani, Faruk Ahmed, Martin Arjovsky, Vincent Dumoulin, and Aaron Courville. Improved training of wasserstein gans. *arXiv preprint arXiv:1704.00028*, 2017.
- Irina Higgins, Loïc Matthey, Arka Pal, Christopher Burgess, Xavier Glorot, Matthew Botvinick, Shakir Mohamed, and Alexander Lerchner. beta-vae: Learning basic visual concepts with a constrained variational framework. In *5th International Conference on Learning Representations, ICLR 2017, Toulon, France, April 24-26, 2017, Conference Track Proceedings*. OpenReview.net, 2017. URL <https://openreview.net/forum?id=Sy2fzU9gl>.

- Justin Johnson, Alexandre Alahi, and Li Fei-Fei. Perceptual losses for real-time style transfer and super-resolution. In *European conference on computer vision*, pages 694–711. Springer, 2016.
- Tero Karras, Timo Aila, Samuli Laine, and Jaakko Lehtinen. Progressive growing of gans for improved quality, stability, and variation. *arXiv preprint arXiv:1710.10196*, 2017.
- Tero Karras, Samuli Laine, and Timo Aila. A style-based generator architecture for generative adversarial networks. In *Proceedings of the IEEE/CVF Conference on Computer Vision and Pattern Recognition*, pages 4401–4410, 2019.
- Tero Karras, Samuli Laine, Miika Aittala, Janne Hellsten, Jaakko Lehtinen, and Timo Aila. Analyzing and improving the image quality of stylegan. In *Proceedings of the IEEE/CVF Conference on Computer Vision and Pattern Recognition*, pages 8110–8119, 2020.
- Hyunjik Kim and Andriy Mnih. Disentangling by factorising. In *International Conference on Machine Learning*, pages 2649–2658. PMLR, 2018.
- Diederik P Kingma and Prafulla Dhariwal. Glow: Generative flow with invertible 1x1 convolutions. *arXiv preprint arXiv:1807.03039*, 2018.
- Diederik P Kingma and Max Welling. Auto-encoding variational bayes. *arXiv preprint arXiv:1312.6114*, 2013.
- Ivan Kobyzev, Simon Prince, and Marcus Brubaker. Normalizing flows: An introduction and review of current methods. *IEEE Transactions on Pattern Analysis and Machine Intelligence*, 2020.
- Z. Lin, K. K. Thekumparampil, G. Fanti, and Sewoong Oh. Infogan-cr: Disentangling generative adversarial networks with contrastive regularizers. *ArXiv*, abs/1906.06034, 2019.
- Xudong Mao, Qing Li, Haoran Xie, Raymond YK Lau, Zhen Wang, and Stephen Paul Smolley. Least squares generative adversarial networks. In *Proceedings of the IEEE international conference on computer vision*, pages 2794–2802, 2017.
- Takeru Miyato, Toshiki Kataoka, Masanori Koyama, and Yuichi Yoshida. Spectral normalization for generative adversarial networks. *arXiv preprint arXiv:1802.05957*, 2018.
- Aamir Mustafa, Aliaksei Mikhailiuk, Dan Andrei Iliescu, Varun Babbar, and Rafal K Mantiuk. Training a better loss function for image restoration. *arXiv preprint arXiv:2103.14616*, 2021.
- George Papamakarios, Theo Pavlakou, and Iain Murray. Masked autoregressive flow for density estimation. *arXiv preprint arXiv:1705.07057*, 2017.
- Omkar M. Parkhi, Andrea Vedaldi, and Andrew Zisserman. Deep face recognition. In Mark W. Jones Xianghua Xie and Gary K. L. Tam, editors, *Proceedings of the British Machine Vision Conference (BMVC)*, pages 41.1–41.12. BMVA Press, September 2015. ISBN 1-901725-53-7. doi:[10.5244/C.29.41](https://dx.doi.org/10.5244/C.29.41). URL <https://dx.doi.org/10.5244/C.29.41>.
- Alec Radford, Luke Metz, and Soumith Chintala. Unsupervised representation learning with deep convolutional generative adversarial networks. *arXiv preprint arXiv:1511.06434*, 2015.
- Elad Richardson, Yuval Alaluf, Or Patashnik, Yotam Nitzan, Yaniv Azar, Stav Shapiro, and Daniel Cohen-Or. Encoding in style: a stylegan encoder for image-to-image translation. *arXiv preprint arXiv:2008.00951*, 2020.
- Yujun Shen, Jinjin Gu, Xiaoou Tang, and Bolei Zhou. Interpreting the latent space of gans for semantic face editing. In *Proceedings of the IEEE/CVF Conference on Computer Vision and Pattern Recognition*, pages 9243–9252, 2020a.
- Yujun Shen, Ceyuan Yang, Xiaoou Tang, and Bolei Zhou. Interfacegan: Interpreting the disentangled face representation learned by gans. *IEEE Transactions on Pattern Analysis and Machine Intelligence*, 2020b.
- Shane D Sims. Frequency domain-based perceptual loss for super resolution. In *2020 IEEE 30th International Workshop on Machine Learning for Signal Processing (MLSP)*, pages 1–6. IEEE, 2020.
- Laurens Van der Maaten and Geoffrey Hinton. Visualizing data using t-sne. *Journal of machine learning research*, 9(11), 2008.
- Tianyi Wei, Dongdong Chen, Wenbo Zhou, Jing Liao, Weiming Zhang, Lu Yuan, Gang Hua, and Nenghai Yu. A simple baseline for stylegan inversion. *arXiv preprint arXiv:2104.07661*, 2021.
- Yinghao Xu, Yujun Shen, Jiapeng Zhu, Ceyuan Yang, and Bolei Zhou. Generative hierarchical features from synthesizing images. *arXiv e-prints*, pages arXiv–2007, 2020.
- Richard Zhang, Phillip Isola, Alexei A Efros, Eli Shechtman, and Oliver Wang. The unreasonable effectiveness of deep features as a perceptual metric. In *Proceedings of the IEEE conference on computer vision and pattern recognition*, pages 586–595, 2018.
- H. Zhao, O. Gallo, I. Frosio, and J. Kautz. Loss functions for image restoration with neural networks. *IEEE Transactions on Computational Imaging*, 3(1):47–57, 2017. doi:[10.1109/TCI.2016.2644865](https://doi.org/10.1109/TCI.2016.2644865).
- Yutong Zheng, Yu-Kai Huang, Ran Tao, Zhiqiang Shen, and Marios Savvides. Unsupervised disentanglement of linear-encoded facial semantics. *arXiv preprint arXiv:2103.16605*, 2021.

## 7 Supplementary Material

The supplementary material is organized as follows: Section 7.1 illustrates the inconsistency between the perceptual and the latent euclidean distance. In section 7.2, we visualize the linear separation of the attributes in the latent space. Finally, section 7.3 details the ablation study.

### 7.1 Perceptual distance vs Latent distance

In this section, we illustrate the inconsistency between the latent Euclidean distance and the perceptual distance in the image space.

**Implementation details** Real NVP consists of 13 coupling layers and is trained with the objective (3).  $\lambda_d=10$ . The latent distance is the MSE and the Perceptual one is VGG16 pretrained on Imagenet. During training and test, the perceptual distance is rescaled (multiplied by 10) to be in the same scale as the latent distance. We randomly sampled 600 pairs of latent codes (images are from the Celeba-HQ dataset and were encoded using the pretrained encoder) and computed the latent distance in both spaces ( $\mathcal{W}^+$ ,  $\mathcal{W}^*$ ) and the perceptual distance of the corresponding image pairs.

**Results** As we can see in Figure 5 and 6, the latent distance is not consistent with the perceptual one in  $\mathcal{W}^+$ . In  $\mathcal{W}^*$  the latent distance is more similar to the perceptual one and closer to the ideal distance (equality between the two distances).

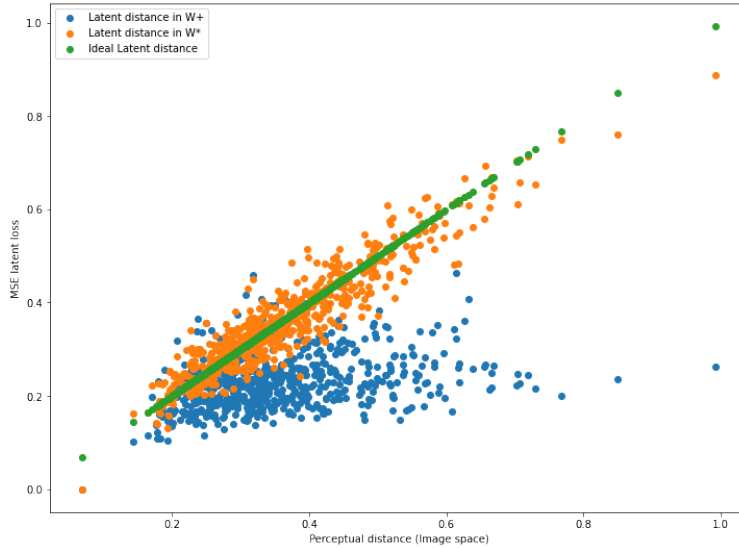


Figure 5: An illustration of the inconsistency between the latent and the perceptual distance: each point represents pair of images. The latent distance is computed in  $\mathcal{W}^+$  (Blue) and  $\mathcal{W}^*$  (Orange). The green diagonal line represents the ideal relationship between the two distances.

### 7.2 Linear Separation of the attributes

In this section we use t-SNE <sup>2</sup> Van der Maaten and Hinton [2008] to visualize the negative and positive examples for some attributes in both latent spaces (*i.e.*  $\mathcal{W}^*$  and  $\mathcal{W}^+$ ), embedded onto the 2D plane. The training setup is the same as in Section 4.1 and 4.3.1. The dataset is composed of 2000 latent codes averaged over the 18 dimensions.

From Figure 7, one can easily visualise that negative and positive attributes are more linearly separated in  $\mathcal{W}^*$  than in  $\mathcal{W}^+$ .

### 7.3 Ablation Study

In this section, we detail the quantitative and qualitative ablation study.

<sup>2</sup>Used from scikit-learn library with default parameters: <https://scikit-learn.org/stable/modules/generated/sklearn.manifold.TSNE.html>



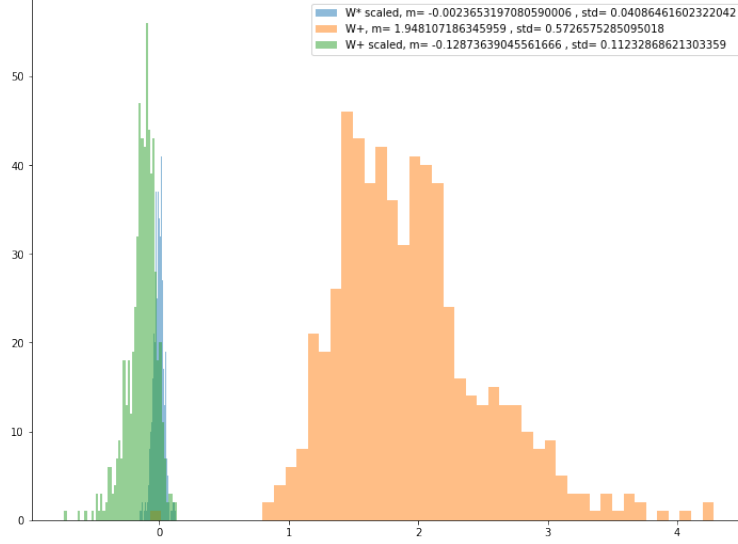


Figure 6: An illustration of the inconsistency between the latent and the perceptual distance: the histograms show the difference between the perceptual and the latent distance of 600 pair of images. The latent distance is computed in  $\mathcal{W}^+$  (Green),  $\mathcal{W}^+$  without rescaling the perceptual loss (Orange) and  $\mathcal{W}^*$  (Blue).

### 7.3.1 Quantitative evaluation

In this section, we investigate the effect of some design choices. The setup is the same as in Section 4.1 except when stated otherwise. We do not rescale the perceptual distance. We analyse 4 experiments which differ from the main setup with the following; H (High model capacity, 13 coupling layers), L (Low model capacity, 4 coupling layers), R (using random classifier, 13 coupling layers), 1R (using one random classifier with 1 linear layer for all the attributes at once, 13 coupling layers). From Table 3:

- Model Capacity (H/L): We can notice that higher model capacity gives slightly better improvement for attribute separation and latent distance unfolding.
- Random Classifier (R): Better initialization of the classifier leads to slightly better separation.
- One Random Classifier (1R): Using one classifier for all the attributes gives worse separation, which can be explained by the capacity of the model (1 layer vs 40 layers) or the fact that optimizing for one class is easier than for 40 classes (even though all the classifiers are optimized jointly). In addition, we noticed that the classification loss is smaller compared to using 40 classifiers, which may have an equivalent effect as multiplying the unfolding loss by a higher  $\lambda_d$ , thus the distance unfolding results are better.

Space	Linear separation			Disentanglement			Dist. Unfolding	
	Min Class. Acc $\uparrow$	Max Class. Acc $\uparrow$	Avg. Class. Acc $\uparrow$	D $\uparrow$	C $\uparrow$	I $\downarrow$	Mean $\downarrow$	STD $\downarrow$
$\mathcal{W}^+$	0.635	0.979	0.834	0.59	0.43	0.30	1.95	0.970
$\mathcal{W}^*$ (H)	<b>0.787</b>	0.991	<b>0.928</b>	<b>0.82</b>	<b>0.56</b>	0.27	0.17	0.15
$\mathcal{W}^*$ (L)	0.777	<b>0.992</b>	0.913	0.81	0.55	<b>0.26</b>	0.13	0.14
$\mathcal{W}^*$ (R)	0.654	<b>0.992</b>	0.927	0.80	0.54	0.27	0.25	0.21
$\mathcal{W}^*$ (1R)	0.686	0.988	0.873	0.79	0.55	0.27	<b>0.0004</b>	<b>0.04</b>

Table 3: Ablation study on Celeba-HQ dataset.  $\mathcal{W}^*$  (H) and  $\mathcal{W}^*$  (L) refer to Real NVP model with 13 and 4 coupling layers, respectively. For  $\mathcal{W}^*$  (R) and  $\mathcal{W}^*$  (1R) the classification model is not pretrained and one classification model for all attributes is used for the latter. Using one classification model per attribute gives significantly better results than using one model. Model capacity and weight initialization of the classification model are less significant.

Note that, scaling the perceptual distance is in favor of the distance unfolding, thus the linear attributes separation and disentanglement results are better than the one in the paper.

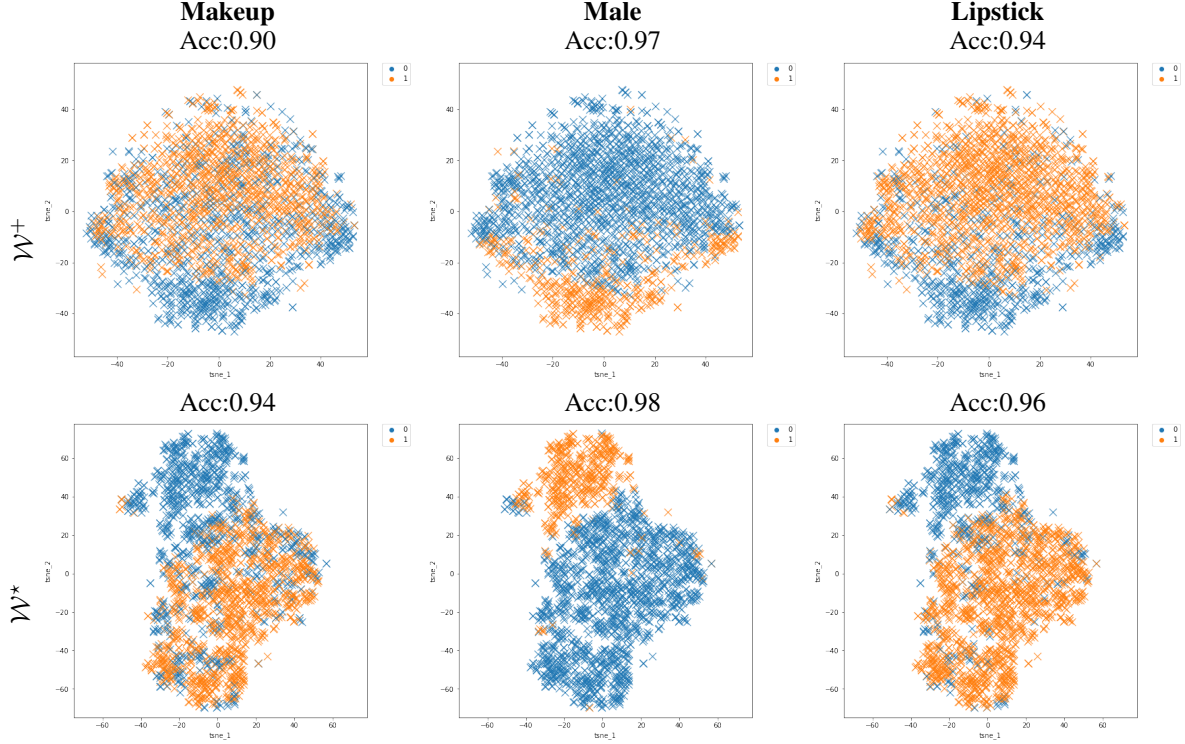


Figure 7: t-SNE visualization in  $\mathcal{W}^+$  and  $\mathcal{W}^*$ : the classification accuracy is shown at the top (Acc). the 2D embedding enables to visualize that the attributes are better linearly disentangled in  $\mathcal{W}^*$ .

### 7.3.2 Qualitative evaluation

In this section, we will investigate the effect of different losses used for image editing. The same setup is used as in Section 4.3.2 except that we fix the editing step to 10 in  $\mathcal{W}^*$  (except we put it 6 for  $\mathcal{W}_a^*$ ). We compare the following choices:

- $\mathcal{W}_a^*$ , where  $T$  is trained only with the attribute separation loss eq. (2),
- $\mathcal{W}_a^*$ -ID:  $\mathcal{W}_a^*$  with the identity preservation loss,
- $\mathcal{W}_a^*$ -ID\*:  $\mathcal{W}_a^*$  with lower weight for the identity loss  $\lambda_{ID} = 0.1$ ,
- $\mathcal{W}_a^*$ -ID $^\dagger$ :  $\mathcal{W}_a^*$ -ID with random classifiers.

From Figure 8, 9, 10, we can conclude that:

1. The identity loss helps to preserve the identity after editing (Row 2 vs 3, 4 and 5). In addition, there is a trade-off between preserving the identity and the amount of editing effect. Specifically, increasing  $\lambda_{ID}$  lead to lower editing effect (Row 3 vs 5).
2. The latent distance unfolding loss has negligible effect on editing (Row 3 vs 6).
3. Pretraining the classifiers does not seem to improve the editing results.

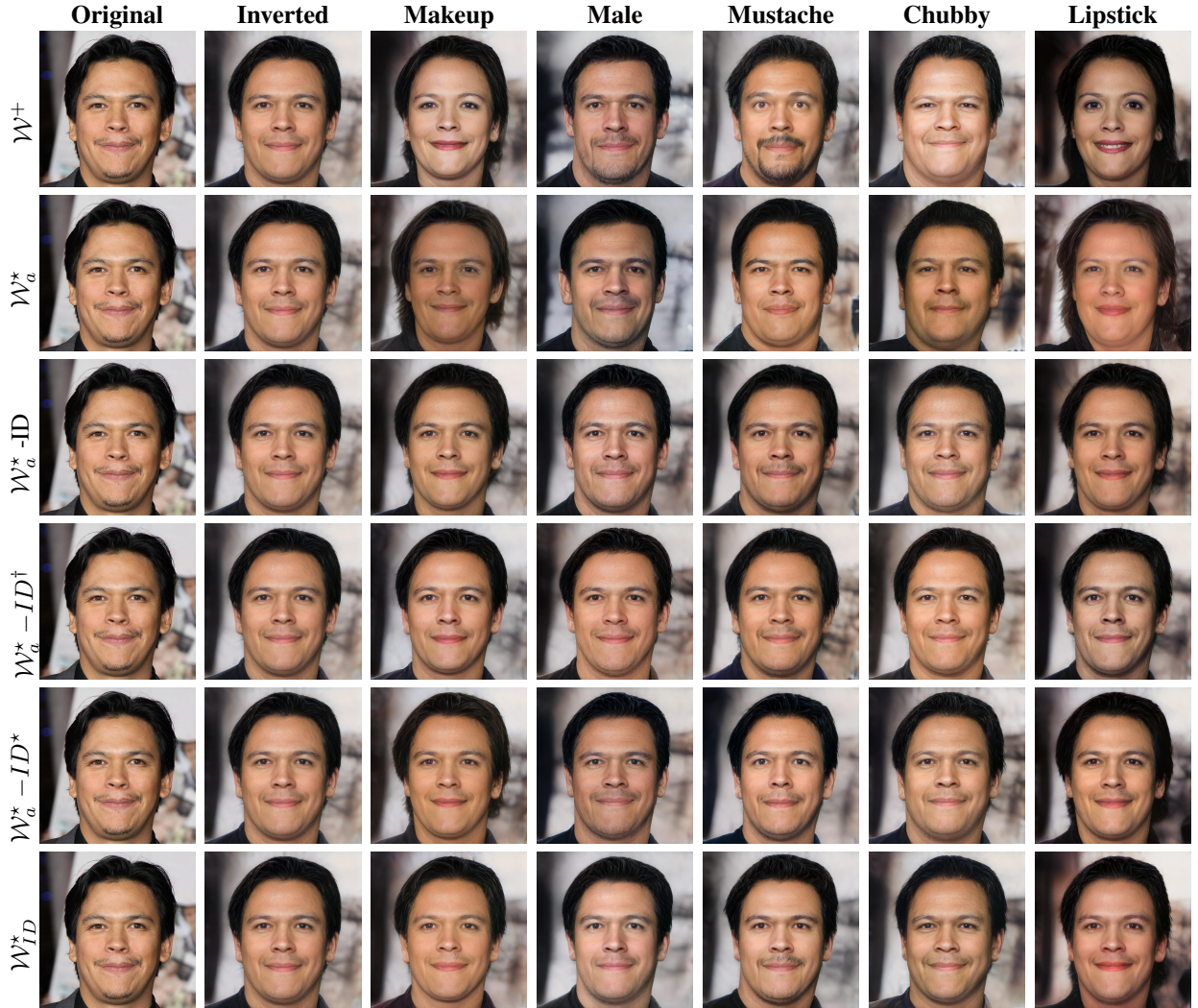


Figure 8: Ablation study: Image editing using InterFaceGAN.



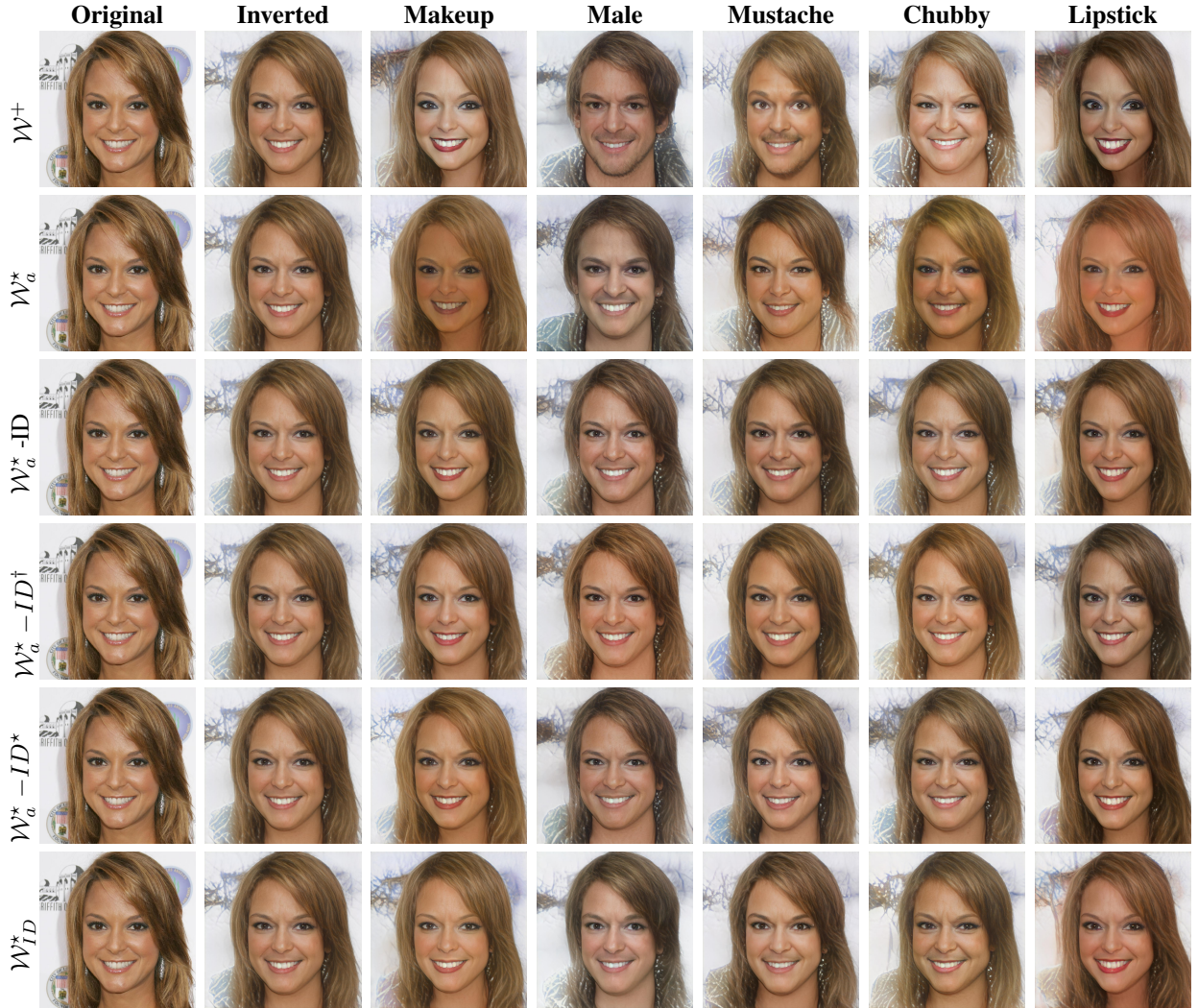


Figure 9: Ablation study: Image editing using InterFaceGAN.

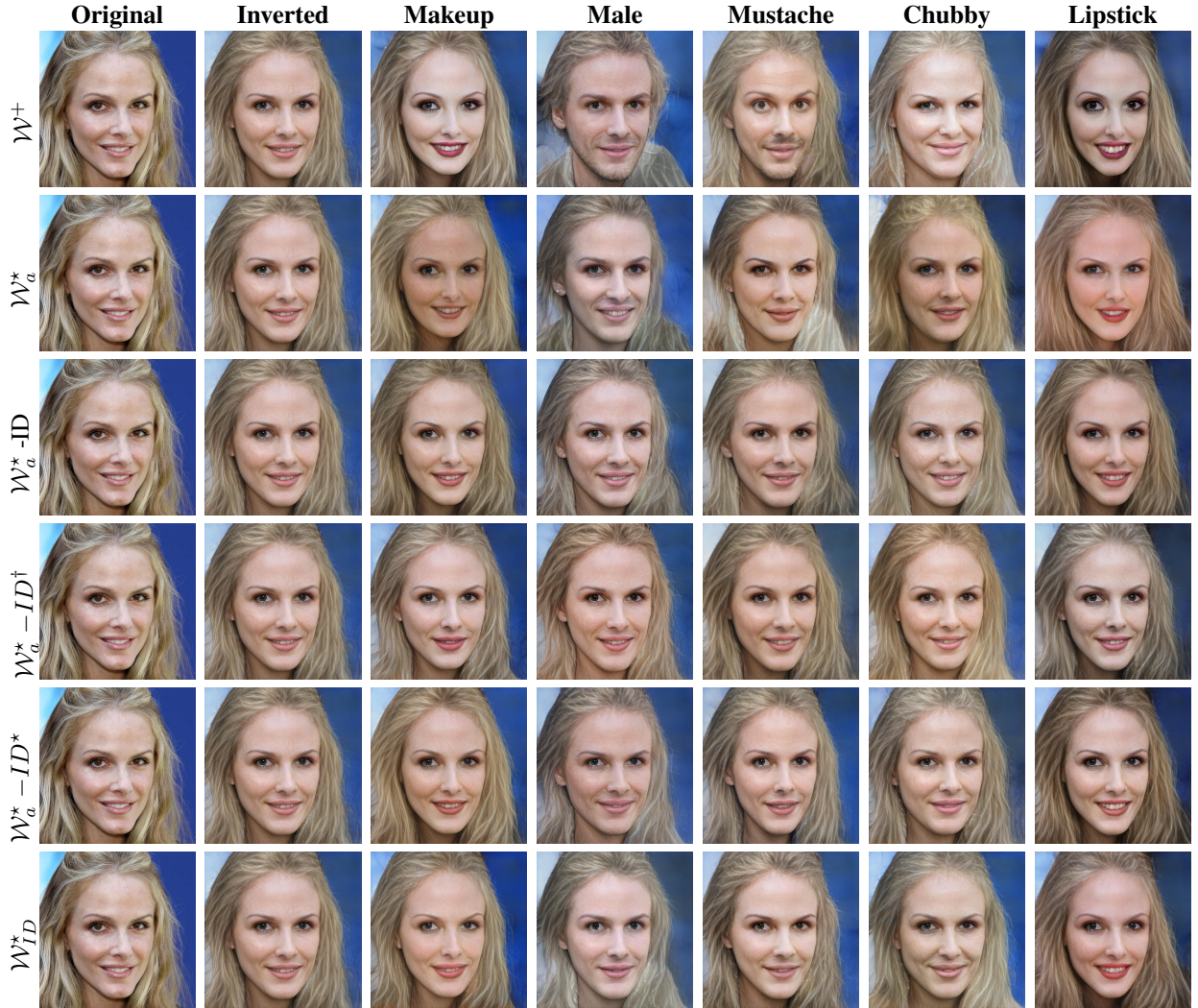


Figure 10: Ablation study: Image editing using InterFaceGAN.





Figure 11: Image editing at resolution  $1024^2$  using InterFaceGAN in  $\mathcal{W}^+$  and  $\mathcal{W}_{ID}^*$ : The images are projected in the latent space of StyleGAN2, then the latent codes are moved in the direction that corresponds to changing one facial attribute. The editing is better in terms of attributes disentanglement in the new learned space ( $\mathcal{W}_{ID}^*$ ) compared to the editing done in the original latent space ( $\mathcal{W}^+$ ). Our method also leads to a better identity preservation.